arXiv:1711.01352v1 [physics.chem-ph] 3 Nov 2017

Experimentally Quantifying Anion Polarizability at the Air/Water Interface

Yujin Tong,* Igor Ying Zhang, and R. Kramer Campen

Fritz Haber Institute of the Max Planck Society, 14195 Berlin, Germany

E-mail: tong@fhi-berlin.mpg.de

Phone: +49 (0)30 84135220. Fax: +49 (0)30 84135206

Abstract

The adsorption of anions from aqueous solution on the air/water interface controls important heterogeneous chemistry in the atmosphere and is thought to have similar physics to anion adsorption at hydrophobic interfaces more generally. Starting in the mid 1990s a wide variety of theoretical and experimental approaches have found the adsorption of large, polarizable anions is thermodynamically favorable. While the qualitative insight is clear, determining the role of polarizability in adsorption has proven surprisingly challenging: simple physical models make clear that nonpolarizable anions will not adsorb, but trends in anion adsorption are difficult to rationalize based on polarizability and, in some theoretical approaches, adsorption is observed without change in anion polarization. Because there are no *experimental* studies of interfacial anion polarizability, one possible explanation for this apparent contradiction is that theoretical descriptions suffer from systematic error. In this study we use interface specific nonlinear optical spectroscopy to extract the spectral response of the interfacial ClO_4^- anion. We find that (i) the interfacial environment induces a break in symmetry of the anion due to its solvation anisotropy (ii) the Raman depolarization ratio, a measure of the ratio of the change in two components of ClO_4^-'s polarizability tensor

with change in nuclear positions, is $> 2\times$ larger than its value in the adjoining bulk phase and interfacial concentration dependent and (iii) using a simple theoretical description we find that our measured changes in depolarization ratio are consistent with known changes in surface potential and tension with small changes in bulk ClO_4^- concentration. The notion that interfacial anion polarizability differs from that in bulk, and that this polarizability is coverage dependent, is not accounted for in any current theoretical treatment of ions at the air/water interface. Accounting for such effects in classical models or validating their reproduction in *ab initio* would be a valuable next step in understanding the physics of anion adsorption at the air/water interface.

Introduction

The adsorption of anions on hydrophobic interfaces controls important chemistry on aerosol surfaces and determines the stability of proteins, colloids and foams in a wide variety of environmental, physiological and engineered settings. Anion adsorption on the air/water interface, the paradigmatic hydrophobic surface, has been particularly well studied.[1–11] Perhaps the simplest question one can ask of this system is do anions tend to exist at higher or lower concentrations at the air/water interface than in the adjoining bulk aqueous phase: is the adsorption of anions at the air/water interface thermodynamically favorable?

In principle measurements of surface tension of the air/water interface as a function of bulk ionic strength provide such insight. Many decades of such measurements have confirmed that surface tensions of aqueous salt solutions increase with increasing ionic strength, those of acids decrease, and that the magnitude of the effect depends strongly on anion and only weakly on cation.[1,12–16] Historically the first two observations were rationalized by Wagner, Onsager and Samras (WOS) in their extension of the Debye-Hückel theory of bulk aqueous electrolytes to interfaces. Within this description anions tend to be *excluded* from the air/water interface because exposure to a low dielectric phase leads to an enormous, unfavorable increase in electrostatic self-energy.[17,18] While qualitatively consistent with surface tension measurements,

this approach does not explain the strong dependence of the size of the measured effect on anion type, nor the weak dependence on cation.

Spurred by measured reaction rates of gas phase species with solvated halogen anions in atmospheric aerosols that were too fast to be explained unless anions exist at aersol surfaces in *higher* concentration than in the adjoining bulk phase,[19] subsequent work – simulation using classical polarizable force fields, various surface sensitive spectroscopies,[2,11,20,21] dielectric continuum theory,[22–25] and properly parameterized fixed charge models[26] – has shown this Debye-Hückel inspired view to be incorrect. Large polarizable anions tend to exist in higher concentrations at the air/water interface than in the adjoining bulk liquid. While the qualitative picture is clear, understanding of quantitative trends in anion adsorption, *e.g.* why does I^- adsorb more strongly than Cl^-, and gaining atomically resolved insight into the driving force of anion adsorption has proven extremely challenging.

Central to this challenge is resolving the contribution of ion polarizability to the free energy of ion adsorption. Within the context of WOS theory ions are represented as nonpolarizable point charges. As illustrated by Levin for an idealized anion, it is this lack of polarizability that leads to the large penalty in electrostatic self-energy for anion adsorption in the WOS model: for an ideal, polarizable anion essentially all charge density shifts towards the aqueous phase as the ion approaches the interface.[23] While it is thus clear that polarizability must play a role in the thermodynamic driving force of ion adsorption at hydrophobic interfaces, such an idealized model doesn't offer a molecularly resolved or quantitative view of *how*. Initial attempts to describe ion adsorption in classical simulations concluded that explicit description of ion polarizability was critical and that the relative surface propensity of different ions was proportional to their polarizability and radius (*i.e.* large, soft, polarizable anions more favorably adsorb).[4,9] However, a variety of subsequent simulation studies have found that anion adsorption occurs in properly parameterized classical models without explicit description of polarizability, that relative anion polarization (where ion polarization is the product of applied field and polarizability $p = \alpha \cdot E$) does not correlate with both

experimental and simulated trends in ion adsorption propensity, and that simulated interface active anions may be similarly polarized in bulk water and at the interface.[21,26–30] One possible explanation for these conflicting results may lie in the difficulty in simulating the interfacial potential of the (pure) water/air interface[29] (and thus error compensation between ion polarizability and surface potential). A second is that, in general, theoretical approaches describe anion polarizability at interfaces incorrectly because of a lack of suitable experimental data against which classical polarizability models might be parameterized or calculated *ab initio* polarizabilities validated.

This missing experimental data is particularly important because one might expect anion polarizability to change at the air/water interface. For monoatomic species this occurs because electron densities of ions at air/water interfaces must reflect the underlying asymmetry of electron density in the solvent, while for multiatomic anions additionally interface induced changes in nuclear arrangement (*e.g.* bond lengths and angles) might be expected to enhance such effects. Furthermore, because such anion structural change might be expected to change as a function of interfacial potential, and because surface potential of the air/water interface is a function of the ionic strength of the bulk aqueous phase,[14,31] it is possible to imagine that anion polarizability at interfaces may be a *function* of bulk ionic strength.

To find an experimental observable of *interfacial* anion polarizability, it is useful to first consider how one might characterize ion polarizability in bulk liquid H_2O. The Raman depolarization ratio (ρ) is one such useful experimental constraint. Given an isotropic distribution of ions in liquid water and a molecular coordinate system (a,b,c) in which a (or b) is taken to be perpendicular to the net deformation of a particular normal mode and c parallel, one writes:[3]

$$\rho = \frac{\mathrm{I}_\perp}{\mathrm{I}_\parallel} = \frac{3}{4 + 5\left(\frac{1+2R}{R-1}\right)^2} \tag{1}$$

where $\mathrm{I}_\perp$ and $\mathrm{I}_\parallel$ are the intensity of inelastic scattered light measured perpendicular and parallel to the, plane polarized incident field and $R = \frac{\partial\alpha^{(1)}_{aa}/\partial Q}{\partial\alpha^{(1)}_{cc}/\partial Q}$. That is the Raman response

of a particular mode can be quantitatively related to the change in the symmetry of the molecules polarizability tensor as the molecule is deformed in the mode's characteristic manner. Given this definition of ρ is it perhaps unsurprising that several studies have shown that the ability to calculate the Raman response of mode that are strongly coupled to the environment is a sensitive test of the accuracy of the polarizability model employed.[33,34] Because spontaneous Raman is not interface-specific it is generally not possible to extract the ρ of *interfacial* anions. Clearly if we could, however, this observable could provide the sort of experimental constraint we seek.

Vibrationally resonant Sum Frequency (VSF) spectroscopy is a nonlinear optical, laser-based technique in which pulsed infrared and visible lasers are spatially and temporally overlapped at an interface and the output at the sum of the frequencies of the two incident beams monitored. The emitted VSF field is interface specific by its symmetry selection rules and a spectroscopy because as one tunes the frequency of one of the incident fields (in this case the infrared (ir)) in resonance with an optically accessible transition the intensity of the emitted sum frequency field ($\mathrm{I_{sf}}$) increases by several orders of magnitude. Much prior work has shown that the intensity of the measured sum frequency response at a frequency ω is proportional to the change in polarizability (α_{ab}) and dipole (μ_c) with motion along the normal mode of frequency ω:[5]

$$\mathrm{I_{sf}} \propto \chi^{(2)}_{ijk} \propto \beta^{(2)}_{abc} \propto -\frac{1}{2\epsilon_0\omega}\frac{\partial\alpha^{(1)}_{ab}}{\partial Q}\frac{\partial\mu_c}{\partial Q} \tag{2}$$

in which $\chi^{(2)}_{ijk}$ is the macroscopic nonlinear susceptibility in the lab coordinate system (ijk), $\beta^{(2)}_{abc}$ the molecular hyperpolarizability and both are second rank tensors. Because by varying experimental conditions, *i.e.* beam incident angles and field polarizations, one can selectively probe different components of $\beta^{(2)}$, a correctly chosen ratio of intensities allows the direct measurement of $R = \frac{\partial\alpha^{(1)}_{aa}/\partial Q}{\partial\alpha^{(1)}_{cc}/\partial Q}$, and thus the possibility of extracting the Raman depolarization ratio of anions with interfacial specificity. That is, by comparing measurements of ρ for an

anion in solution and at the air/water interface experimental estimates of anion polarizability anisotropy at aqueous interfaces (and the change in anion polarizability anisotropy on moving from bulk liquid water to the aqueous interface) are possible.

The perchlorate anion (ClO_4^-) has tetrahedral (T_d) symmetry in bulk liquid H_2O and a favorable free energy of adsorption at the air/water interface.[9,36] Here, using VSF spectroscopy, we probe two Cl-O modes of the perchlorate anion at the air/water interface and show (i) that the T_d symmetry of the ClO_4^- anion in bulk water is lifted at this interface: the ClO_4^-'s ν_1 mode, that is IR inactive in bulk, is now active, and (ii) that the Raman depolarization ratio of the ν_1 mode increases monotonically, and by more than $2\times$, with increasing bulk concentration. Put another way, the polarizability tensor of interfacial ClO_4^- grows increasingly anisotropic with increasing interfacial population. Using a simple computational model we show that the increase in polarizability anisotropy with increasing bulk concentration we observe in experiment can be quantitatively related to increases in interfacial field (consistent with prior measurements of concentration dependent surface potential[37]), ClO_4^- dipole, and relative bond length of one Cl-O bond with respect to the other three with increasing concentrations of bulk $HClO_4$. Quantitative theoretical insights into the driving force of anion adsorption at the air/water interface, and specific ion effects more generally, require accurate calculation of ion polarizability at aqueous interfaces. The results of this study are the first, of hopefully many, experimental observations of this ionic property.

Results and discussion

Figure 1(a) shows the VSF spectra from the air/0.6 M $HClO_4$ solution interface measured under the *ssp* (*s*-polarized SF, *s*-polarized visible, and *p*-polarized IR) (black circles) and *ppp* (red squares) polarization combinations. There are two resonances apparent in this frequency range. Fitting both spectra simultaneously with the Lorentzian lineshape model described in the methods section results in resonances centered at 935 and 1110 cm^{-1} (Figure 1(b) dotted

lines) *.

Because both spectral features are absent in pure water, and are spectrally separated from resonances of water or likely impurities, they can be straightforwardly assigned by reference to Raman and IR measurements of bulk aqueous perchloric acid and perchlorate salt solutions.[6,36,40] In brief, the ClO_4^- anion has four normal modes apparent in calculation: the ν_1 at 930, the ν_2 at 450, the ν_3 at 1100 and the ν_4 at 620 cm^{-1}. All four are Raman active at all concentrations in bulk aqueous solution but the ν_1 and ν_2 are only apparent in IR absorption spectra at bulk concentrations greater than $\approx$ 11 M. This observation is a straightforward consequence of anion symmetry: at bulk concentrations below 11 M the ClO_4^- anion has T_d symmetry (under which condition ν_1 and ν_2 are IR inactive) and at sufficiently high concentrations this symmetry is broken: either by ion pairing or, in the case of $HClO_4$, by the presence of molecular acid. If we assign the resonance apparent in Figure 1(b) at 935 cm^{-1} to the ν_1 mode and that apparent at 1110 cm^{-1} to the ν_3, we are left with an apparent incongruity. As shown in equation 2, VSF activity requires that a mode must be *both* IR *and* Raman active. This implies the ClO_4^- anion must lose its T_d symmetry at the air/water interface at concentrations that are at least 15$\times$ lower than those at which T_d symmetry is lifted in bulk.

We imagine three possible mechanisms for the loss of T_d symmetry: consistent with recent work on other strong acids, molecular $HClO_4$ may exist at the air/water interface at concentrations dramatically lower than in bulk,[41] ClO_4^- may no longer have tetrahedral symmetry due to ion pairing, or it may not have tetrahedral symmetry due to, more general, solvation anisotropy at the interface. We tested the first possibility by collecting spectra from 0.6 M solutions of $NaClO_4$. For this a similarly intense ν_1 feature is observed suggesting the likely cause of T_d symmetry lifting is not molecular acid (see Electronic Supplementary

*It is clear from inspection that the apparent baseline of the spectrum is higher on the low than high frequency side of the data shown in Figure 1. We have previously showed that the libration of water at the air/water interface is a broad spectral feature centered at 834 cm^{-1} (*i.e.* well outside the spectral window of the current study).[1] In performing the global fit of the data in Figure 1 we included the libration as described in the SI.

Information for data).

To evaluate the possibility of T_d symmetry lifting due to ion pairing, it is necessary to understand how ion pairing might be expected to influence the ν_1 and ν_3 spectral response. In bulk solutions of perchlorate salts at concentrations above 1 M the center frequency of perchlorate's ν_3 mode has been observed to continuously shift as a function of concentration.[42] This concentration dependent spectral evolution has been assigned to the formation of weak, solvent-separated ion pairs. As mentioned above, in this concentration range the ν_1 mode is infrared inactive. At still higher concentrations in bulk water, > 11 M, perchlorate's degenerate modes, *i.e.* ν_2, ν_3 and ν_4, have been observed to split due to contact ion pair formation, where the degree of splitting is a function of the extent to which symmetry is broken.[42,43]

As is discussed in detail below (see Figure 2 for data) at bulk concentrations lower than 1 M $HClO_4$ the ν_1 mode is clearly VSF (and thus IR) active, the ν_3 spectral response is quantitatively reproduced with a single center frequency and line width: splitting or frequency shift of the ν_3 resonance is not required to describe our data. We therefore conclude that neither contact nor solvent separated ion pair formation explains the lifting of T_d symmetry. Given that VSF spectra collected at bulk concentrations below 1 M $HClO_4$ are consistent with formation of neither weak, solvent separated ion pairs nor contact ion pairs, we conclude that the lifting of T_d symmetry for interfacial ClO_4^- (and thus the IR and VSF activity of the ν_1 mode) must be the result of the intrinsic anisotropy of the solvation environment at the air/water interface: solvation anisotropy must induce sufficient structural deformation in the ClO_4^- anion to lift the bulk T_d symmetry and make the ν_1 mode IR, and VSF, active.

While this qualitative observation of a consequence of structural deformation is important, to make clear connections to theory it would be useful to quantify this deformation, and the resulting change in the perchlorate polarizability tensor. As shown in the Electronic Supplementary Information, given the ν_1 spectral amplitudes extracted from the fit of the *ssp* and *ppp* data in Figure 1(a), and assuming the ClO_4^- anion is oriented such that one

Cl-O points along the surface normal and that the anion has $C_{3\nu}$ symmetry, we can calculate the Raman depolarization ratio, *i.e.* ρ, for perchlorate ions at the interface. The result of this calculation is shown by the solid black line in Figure 1(b). The ratio of spectral amplitudes of the ν_1 *ssp* and *ppp* spectral amplitudes shown in Figure 1(a) suggests a ν_1 ρ of 0.0063 or more than 2× larger than the same quantity for ClO_4^- in bulk.

It is worth emphasizing that the result that interfacial ClO_4^- is significantly larger than bulk is insensitive to the simplifying assumptions required in its calculation. As we show in the Electronic Supplementary Information, assuming the ClO_4^- is oriented with one Cl-O bond at an increasing, nonzero angle with respect to the surface normal leads to slightly *larger* estimates for the depolarization ratio of ν_1 while assuming the symmetry of the ClO_4^- anion has decreased to $C_{2\nu}$ or $C_{\infty\nu}$ leads to quantitatively similar results. Note also that because we measure the *intensity* of the emitted sum frequency light, and not the *field*, our measurements are equally consistent with one Cl-O bond along the surface normal and the remaining three oxygens pointing either towards the bulk liquid or air. Prior theoretical studies imply, at least in the low concentration limit, that the latter configuration is favored.[7,44,45]

As noted above, changes in polarizability must be correlated with changes in anion nuclear structure. As we show in detail in the Electronic Supplementary Information, a simple computational model suggests a ρ of 0.0062 is consistent with a 3% change in Cl-O bond length (for the Cl-O along the surface normal), and a permanent dipole moment of interfacial ClO_4^- of 0.75 Debye (*n.b.* consistent with the absence of IR active ν_1 and ν_2 modes for the ClO_4^- anion in vacuum or in bulk liquid water perchlorate's dipole moment in either bulk phase is below our detection limit). In this manner our experimental observable directly constrains the anisotropy of interfacial perchlorate's polarizability tensor and places quantitative constraints on interfacial ClO_4^- polarization at the air/ water interface.

To gain more insight into the fate of the ClO_4^- anion at the air/water interface we next measured its ν_1 and ν_3 spectral amplitudes as a function of bulk concentration of $HClO_4$ from 0.1 - 0.8 M (higher concentrations lead to qualitative change in the spectral

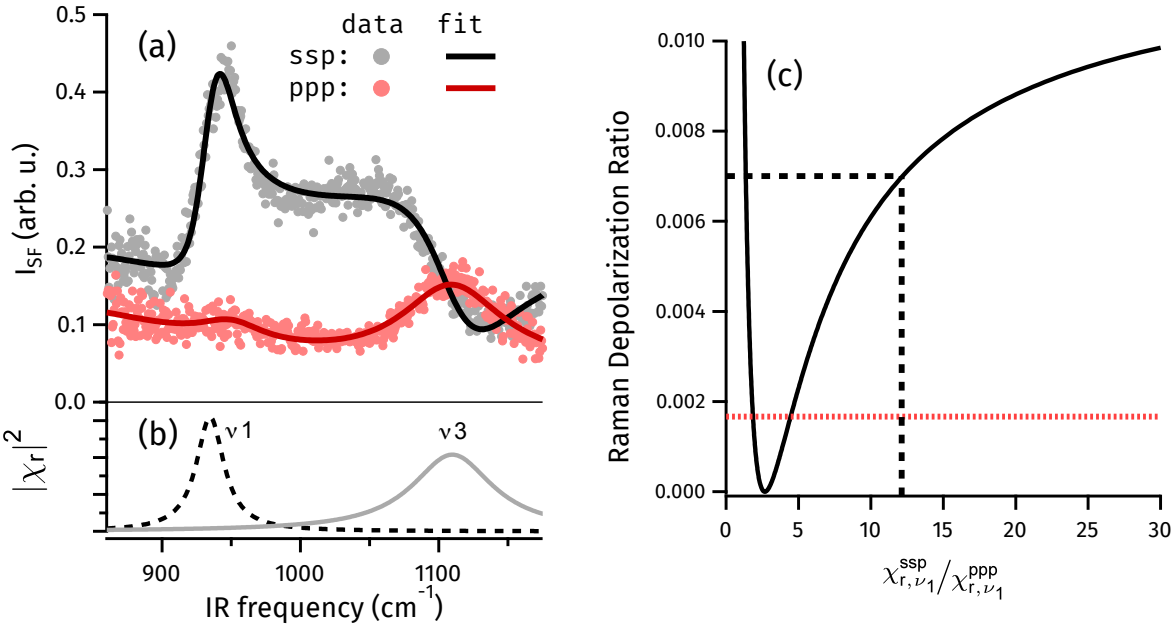

Figure 1: a.) SFG spectrum of 0.6 M $HClO_4$ solution at the air/water interface measured under *ssp* (black traces) and *ppp* (red traces) polarization combinations. Circular symbols are the experimental observations; solid traces are the fit to equation 3; b.) Two components obtained from spectral fit, assigned to ν_1 (A1 symmetry) and ν_3 (F2 symmetry) vibrational modes of perchlorate respectively; c.) Calculated Raman depolarization ratio (black solid line) as a function of the measured VSF peak amplitude ratio ($\chi^{ssp}_{r,\nu_1}/\chi^{ppp}_{r,\nu_1}$); the black dashed line is the result of fitting the data shown in (a), the red dashed line indicates the bulk value reported by prior authors.[6]

response, possibly the result of interface induced ion pairing, as shown in the Electronic Supplementary Information). The concentration dependent spectra collected under the *ssp* polarization condition are shown in Figure 2(a), the concentration dependent *ppp* are plotted in the Electronic Supplementary Information. Global fitting of both sets of data allows the extraction of the $\chi^{ssp}_{r,\nu_1}/\chi^{ppp}_{r,\nu_1}$ ratio as a function of concentration. As shown in Figure 2(b) changing bulk concentrations of $HClO_4$ from 0.1 - 0.8 M leads to a change of this ratio from 8 - 13. Reference to Figure 1 makes clear that this change in spectral amplitude implies an increase in the raman depolarization ratio of ν_1 of 0.004 - 0.007 over the same concentration range. Evidently, with increasing interfacial population, ClO_4^- polarizability grows increasingly anisotropic. Using the same simple computational model discussed above, increasing the depolarization ratio from 0.004 to 0.007 is consistent with an increase in

interfacial field from 139–171 (meV), an elongation in the Cl-O bond along the surface normal of 2.6–3.3 % and a change in ClO_4^- dipole moment from 0.6–0.76.

The relationship between $\chi^{\mathsf{ssp}}_{\mathrm{r},\nu_1}/\chi^{\mathsf{ppp}}_{\mathrm{r},\nu_1}$ and Raman depolarization ratio shown in Figure 1 assumes that the ClO_4^- is orientated such that one Cl-O group points along the surface normal. Applying this analysis to the data shown in Figure 2(a) implicitly assumes that this orientation is concentration independent. Because the ν_1 and ν_3 normal modes are orthogonal, we would expect any concentration dependent change in the orientation of interfacial ClO_4^- to result in significant change in the $\chi^{\mathsf{ssp}}_{\mathrm{r},\nu_1}/\chi^{\mathsf{ssp}}_{\mathrm{r},\nu_3}$ (see Electronic Supplementary Information for a calculation of the size of this effect). As is shown in Figure 2(c) this is not the case. We thus conclude that the orientation of interfacial ClO_4^- is, to within the limits of our sensitivity, over 0.1-0.8 M range in bulk concentration, concentration independent.

Our results suggest the following model for ClO_4^- at the air/water interface: on adsorption ClO_4^- is polarized, *i.e.* it has a nonzero dipole moment, and the polarizability anisotropy changes due to a change in the bond length of the Cl-O that points along the surface normal relative to the three other Cl-O bonds. With increasing interfacial concentrations of ClO_4^- the interfacial field increases, ion polarization increases (the dipole continues to grow) and the polarizability anisotropy continues to increase.

Modern dielectric continuum descriptions, principally developed over the last eight years by Levin and coworkers, largely reproduce experimentally measured changes in surface tension with increasing concentrations of both acids and salts.[24] In this approach anions are treated as spheres whose polarizability and radius are concentration dependent input parameters and whose electrostatic self energy is defined relative to the dielectric constants of, bulk, water and air. Notably the largest disagreements between experiment and theory exist for ClO_4^- solutions (both acids and salts). Levin, dos Santos and coworkers have suggested that this is likely the result of inaccuracies in the estimates of ionic radii for ClO_4^-.[46,47] Our results are consistent with an alternative scenario in which anion polarizability (and ClO_4^- radius) is interfacial concentration dependent. While our results imply the relationship between ClO_4^-

radius and interfacial concentration is monotonic, larger multivalent ions might be expected to have a more complicated interplay between polarizability, structure, dipole and interfacial concentration.

Atomistic simulation studies, whether employing classical or ab-initio potential energy surfaces, have largely reported either potentials of mean force for ion adsorption in the limit of infinite dilution or *brute force* simulations at a fixed ion concentration. As alluded to above, while important and informative these studies suffer from a variety several possible shortcomings. The lack of experimental constraints on polarizability means that there is no experimental parameterization of classical polarizability models and that *ab-initio* treatments of polarizability cannot be validated. To further heighten the challenge the surface potential of pure water is both difficult to measure experimentally and the subject of significant disagreement, (by more than 0.5 V) in simulation treatments.[48] Thus one might expect that inaccuracies in surface potential of the pure water/air interface might, plausibly compensate for inaccuracies in polarizability treatment.

Data of the sort described in this study gives a clear path forward through these challenges. Clearly, given experimental constraints on interfacial anion polarizability, empirical polarizability models can be more accurately parameterized and *ab-initio* treatments validated. Given this validated polarizability model, systematically reducing errors in the calculation of (ion concentration dependent) surface potential is now much more straight forward.

Prior workers have performed studies similar in spirit to those shown here. Miyame, Morita and Ouchi characterized the S-O stretch vibrations of SO_4^{2-}, while Motschmann and coworkers characterized the CN stretch vibrations of the potassium ferricynaide ion, *i.e.* $Fe(CN)_6^{4-}$, as a function of bulk concentration at the air/water interface.[6,10] Consistent with both calculation and other experimental approaches that suggest SO_4^{2-} retains its bulk solvation shell at the air/water interface,[4,49] Miyame, Morita and Ouchi find interfacial SO_4^{2-} to be essentially the same as bulk. In contrast Motschmann and coworkers found that CN modes that were IR inactive in bulk solution were apparent in the VSF spectrum, *i.e.* the

interface induces a change in ferricyanide symmetry as it does for perchlorate. However, presumably because of the more structurally complicated anion, they were unable to quantify the resulting change in the polarizability tensor.

As is clear from equation 2 if a molecules hyperpolarizability is concentration independent it should, in principle, be possible to extract a measurement of anion interfacial density as a function of bulk concentration by plotting the square of the measured SF signal vs. bulk concentration. In a series of studies employing electronically resonant second harmonic measurements of a variety of anions at air/water interface Saykally and co-workers have treated anion hyperpolarizability as concentration independent, fit adsorption isotherms to measurements of SHG signal as a function of bulk concentration, and calculated anion adsorption energies.[5,21] Our results suggest that this type of data needs to be revisited. Because deformation of the perchlorate leads to an *increase* in dipole and polarizability tensor ratio it is clear that, given a VSF spectra collected under the *ssp* polarization condition, using this approach would significantly overestimate adsorption energies (*i.e.* the molecular response of the perchlorate anion would increase with increasing concentration).

In summary, in the current study we have employed VSF spectroscopy and a simple computational model to study the behavior of ClO_4^- at the air/$HClO_4$ solution interface. Consistent with much prior work our observations clearly demonstrate that ClO_4^- is a surface active anion. We significantly extend these prior efforts by demonstrating that the presence of the interface induces deformation of the anion, which cause a bulk forbidden mode to be VSF active due to change in anion symmetry, creates a nonzero dipole moment and leads to a change in the measured polarizability anisotropy. Our results suggest that increasing density of ClO_4^- at the interface leads an increasing interfacial field that both leads to increasing ClO_4^- polarization (*i.e.* increasing ClO_4^- dipole moment), and increasingly anisotropic ClO_4^- polarizability.[4,5,9] Extension of the approach we describe here should allow the possibility of directly quantifying of the elements of ClO_4^- polarizability tensor, rather than just their ratio, and allow straight forward estimate of any thermodynamic significance of the concentration

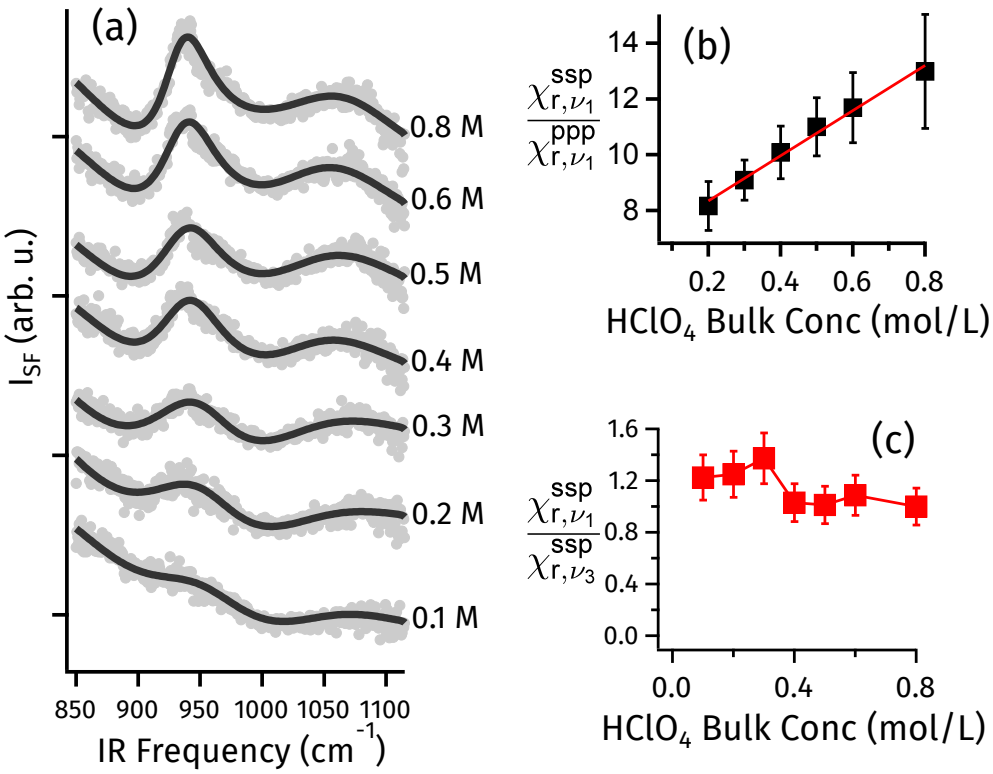

Figure 2: a) VSF spectra as a function of ClO_4^- concentration below 1 M for the *ssp* polarization combinations. Grey dots are data and solid black lines the corresponding fits. b) $\chi^{ssp}_{r,\nu_1}/\chi^{ppp}_{r,\nu_1}$ for the data in a) and the SI illustrating the linearity of this ratio with respect to bulk $HClO_4$ concentration. The uncertainty at each point is extracted from the fits to the data as described in the SI. c) $\chi^{ssp}_{r,\nu_1}/\chi^{ssp}_{r,\nu_3}$ extracted from the data in a) and the SI. Clearly this ratio is essentially constant with respect to bulk concentration of $HClO_4$. As discussed in the text this indicates that the orientation of interfacial ClO_4^- is concentration independent. The straight line is a guide to the eye.

dependent interfacial anion polarizability.

The close connection we describe here between the dipole moment, structure and polarizability of interfacial anions with increasing interfacial field has not, to our knowledge, been previously considered but should be a quite general feature of anion, particularly polyvalent anion, adsorption at hydrophobic interfaces. As such its quantitative reproduction is a prerequisite for simulation approaches that attempt to offer microscopic insight into this phenomena.

Methods

Solution Preparation

$HClO_4$ (Suprapur, 70%, Merck) and $NaClO_4$ (>99.99%, Sigma-Aldrich) were used as received. Solutions with indicated concentration were prepared by diluting the high concentration of $HClO_4$ and $NaClO_4$ in ultrapure H_2O (18.3 MΩ·cm, Milli-Q, Millipore). All solutions are prepared freshly before each measurement to limit degradation or contamination. VSF measurements in the C-H stretching and C=O region were employed to judge the quality of the solutions.

VSF Measurement and Spectral Modeling

The VSF spectrometer employed for the current measurement, and in particular its power at long infrared wavelengths has been described in detail in our previous studies.[1,50] In the interest of brevity only a brief description that pertinent to this measurement will be given here. The IR beam was generated from a commercial optical parametric amplifier (HE-TOPAS, Light Conversion) with a difference frequency generation (DFG) module. The full width half maximum (FWHM) of the beam at frequency region between 600–1200 cm^{-1} is typically 300 cm^{-1} with GaSe was used as the DFG crystal. To probe the interfacial Cl-O stretch modes the center frequency of the beam was tuned to ≈ 1000 cm^{-1}. A narrow-band visible (VIS) pulse was produced from a home-made spectral shaper.[50] The beam is centered at 800 nm with a bandwidth of 15 cm^{-1}. The energy per pulse of the IR and VIS at the sample surface was 5.8 and 15.4 μJ respectively. Polarizations and energies of the incident fields at the interface were controlled using $\lambda/2$ plate, polarizer, $\lambda/2$ plate combinations. The two beams propagate in a coplanar fashion and focused on the samples using lenses with focal lengths of 10 and 25 cm and incident angles of $39.5 \pm 0.5°$ and $65 \pm 0.5°$ for the IR and VIS. All measurements were conducted in ambient conditions at room temperature and under the *ssp* (*s*-polarized SF, *s*-polarized visible, and *p*- polarized IR where *p* indicates

polarization in the plane of incidence and *s* polarization orthogonal) and *ppp* polarization condition. Non-resonant signals from a gold thin film were used to correct for the frequency dependent IR intensity. The acquisition time for spectra of the gold reference and samples were 30 and 300 s, respectively.

To quantify the observed VSF spectral response, we adopted a Lorentzian line shape model described and justified in much previous work by us and others.[1,50–53]

$$\mathrm{I_{sf}}(\omega_{\mathrm{sf}}) \propto \left|\chi^{(2)}_{\mathrm{eff}}\right|^2 \propto \left|\left|\chi_{\mathrm{nr}}\right| e^{i\epsilon} + \sum_n \frac{\chi_{\mathrm{r},n}}{\omega_{\mathrm{ir}} - \omega_n + i\Gamma_n}\right|^2 \tag{3}$$

where $\mathrm{I_{sf}}(\omega_{\mathrm{sf}})$ is the normalized VSF intensity, $\chi^{(2)}_{\mathrm{eff}}$ is the effective second order susceptibility, which depends on the experimental geometry, molecular hyperpolarizability and orientation.$|\chi_{\mathrm{nr}}|$ and ϵ are the nonresonant amplitude and phase and $\chi_{\mathrm{r},n}$, ω_n and Γ_n are the complex amplitude, center frequency and line width of the nth resonance.

To actually analyze the data we fit the measured VSF spectrum using the Levenberg-Marquardt algorithm as implemented in the commercial visualization and analysis program Igor Pro (Wavemetrics). Fitting spectra collected at each bulk concentration and polarization with this line shape model results in an underdetermined minimization problem. Because bulk studies suggest that the center frequencies and spectral shape of ClO_4^- solution are concentration independent, we addressed this data by assuming that all spectra collected under a bulk concentration of $HClO_4$ could be described with two resonances, each with a concentration independent line width, center frequency and phase, and a nonresonant amplitude and phase that are also concentration independent. We accounted for the libration tail (only important in the *ssp* spectra) by assuming the libration has the center frequency and line width from our previous study.[1] Details of the analysis, and all the parameters resulting from the fit, are given in the Electronic Supplementary Information.

Acknowledgement

The authors thank Martin Wolf for useful discussions and the Max Planck Society for support of this work.

Electronic Supplementary Information

VSF spectra of 0.6 M perchlorate salt solution, details of line shape analysis and all data fitting results, full description of the theory describing the Raman depolarization ratio and its connection to VSF measurements, calculated dependence of the Raman depolarization ratio on ClO_4^- orientation, calculated dependence of the $\chi^{ssp}_{r,\nu_1}/\chi^{ssp}_{r,\nu_3}$ on ClO_4^- orientation, details of the electronic structure calculation and tables of all calculated results illustrating their independence of basis set.

Author Contributions

YT and RKC designed the study. YT performed the measurements. YT and RKC analyzed the data and wrote the paper. IYZ performed the electronic structure calculations. All authors edited the paper.

References

(1) Weissenborn, P. K.; Pugh, R. J. *J Colloid Interface Sci* **1996**, *184*, 550–563.

(2) Ghosal, S.; Hemminger, J. C.; Bluhm, H.; Mun, B. S.; Hebenstreit, E. L. D.; Ketteler, G.; Ogletree, D. F.; Requejo, F. G.; Salmeron, M. *Science* **2005**, *307*, 563–566.

(3) Cheng, J.; Vecitis, C. D.; Hoffmann, M.; Colussi, A. *J Phys Chem B* **2006**, *110*, 25598–25602.

(4) Jungwirth, P.; Tobias, D. J. *Chem Rev* **2006**, *106*, 1259–1281.

(5) Petersen, P. B.; Saykally, R. J. *Ann Rev Phys Chem* **2006**, *57*, 333–364.

(6) Miyamae, T.; Morita, A.; Ouchi, Y. *Phys Chem Chem Phys* **2008**, *10*, 2010–2013.

(7) Baer, M. D.; Kuo, I.-F. W.; Bluhm, H.; Ghosal, S. *J Phys Chem B* **2009**, *113*, 15843–15850.

(8) Hua, W.; Verreault, D.; Allen, H. C. *J Phys Chem Lett* **2013**, *4*, 4231–4236.

(9) Tobias, D. J.; Stern, A. C.; Baer, M. D.; Levin, Y.; Mundy, C. J. *Annu Rev Phys Chem* **2013**, *64*, 339–359.

(10) Brandes, E.; Karageorgiev, P.; Viswanath, P.; Motschmann, H. *J Phys Chem C* **2014**, *118*, 26629–26633.

(11) Hua, W.; Verreault, D.; Allen, H. C. *J Am Chem Soc* **2015**, *137*, 13920–13926.

(12) Heydweiller, A. *Ann Phys* **1910**, *338*, 145–185.

(13) Randles, J. *Discuss Faraday Soc* **1957**, *24*, 194–199.

(14) Randles, J. E. B.; Schiffrin, D. J. *T Faraday Soc* **1966**, *62*, 2403–2408.

(15) Matubayasi, N.; Matsuo, H.; Yamamoto, K.; Yamaguchi, S.; Matuzawa, A. *J Colloid Interface Sci* **1999**, *209*, 398–402.

(16) Matubayasi, N.; Tsunetomo, K.; Sato, I.; Akizuki, R.; Morishita, T.; Matuzawa, A.; Natsukari, Y. *J Colloid Interface Sci* **2001**, *243*, 444–456.

(17) Wagner, C. *Phys Z* **1924**, *25*, 474–477.

(18) Onsager, L.; Samaras, N. N. T. *J Chem Phys* **1934**, *2*, 528–536.

(19) Knipping, E. M.; Lakin, M. J.; Foster, K. L.; Jungwirth, P.; Tobias, D. J.; Gerber, R. B.; Dabdub, D.; Finlayson-Pitts, B. J. *Science* **2000**, *288*, 301–306.

(20) Padmanabhan, V.; Daillant, J.; Belloni, L.; Mora, S.; Alba, M.; Konovalov, O. *Phys Rev Lett* **2007**, *99*, 086105.

(21) Otten, D. E.; Shaffer, P. R.; Geissler, P. L.; Saykally, R. J. *P Natl Acad Sci USA* **2012**, *109*, 701–705.

(22) Boström, M.; Williams, D. R. M.; Ninham, B. W. *Langmuir* **2001**, *17*, 4475–4478.

(23) Levin, Y. *Phys Rev Lett* **2009**, *102*, 147803.

(24) Levin, Y.; dos Santos, A. P.; Diehl, A. *Phys Rev Lett* **2009**, *103*, 257802.

(25) Wang, R.; Wang, Z.-G. *Phys Rev Lett* **2014**, *112*, 136101.

(26) Netz, R. R.; Horinek, D. *Annu Rev Phys Chem* **2012**, *63*, 401–418.

(27) Caleman, C.; Hub, J. S.; van Maaren, P. J.; van der Spoel, D. *P Natl Acad Sci USA* **2011**, *108*, 6838–6842.

(28) Baer, M. D.; Mundy, C. J. *J Phys Chem Lett* **2011**, *2*, 1088–1093.

(29) Baer, M. D.; Stern, A. C.; Levin, Y.; Tobias, D. J.; Mundy, C. J. *J Phys Chem Lett* **2012**, *3*, 1565–1570.

(30) Sun, L.; Li, X.; Tu, Y.; Agren, H. *Phys Chem Chem Phys* **2015**, *17*, 4311–4318.

(31) Yang, C.; Dabros, T.; Li, D.; Czarnecki, J.; Masliyah, J. H. *J Colloid Interface Sci* **2001**, *243*, 128–135.

(3) Hirose, C.; Akamatsu, N.; Domen, K. *J Chem Phys* **1992**, *95*, 997–1004.

(33) Hamm, P. *J Chem Phys* **2014**, *141*, 184201.

(34) Ito, H.; Hasegawa, T.; Tanimura, Y. *J Phys Chem Lett* **2016**, *7*, 4147–4151.

(5) Lambert, A. G.; Davies, P. B.; Neivandt, D. J. *Appl Spect Rev* **2005**, *40*, 103–145.

(36) Ratcliffe, C.; Irish, D. *Can J Chem* **1984**, *62*, 1134–1144.

(37) Marcus, Y. *Current Opinion In Colloid & Interface Science* **2016**, *23*, 94–99.

(1) Tong, Y.; Kampfrath, T.; Campen, R. K. *Phys Chem Chem Phys* **2016**, *18*, 18424–18430.

(6) Hyodo, S.-a. *Chem Phys Lett* **1989**, *161*, 245–248.

(40) Karelin, A.; Grigorovich, Z. *Spectrochim Acta A* **1976**, *32*, 851–857.

(41) Baer, M. D.; Tobias, D. J.; Mundy, C. J. *J Phys Chem C* **2014**, *118*, 29412–29420.

(42) Chen, Y.; Zhang, Y.-H.; Zhao, L.-J. *Phys Chem Chem Phys* **2004**, *6*, 537–542.

(43) Ritzhaupt, G.; Devlin, J. P. *J Chem Phys* **1975**, *62*, 1982–1986.

(44) Ottosson, N.; Vácha, R.; Aziz, E. F.; Pokapanich, W.; Eberhardt, W.; Svensson, S.; Öhrwall, G.; Jungwirth, P.; Björneholm, O.; Winter, B. *The Journal of Chemical Physics* **2009**, *131*, 124706.

(45) Hey, J. C.; Smeeton, L. C.; Oakley, M. T.; Johnston, R. L. *J Phys Chem A* **2016**, *120*, 4008–4015.

(46) dos Santos, A. P.; Diehl, A.; Levin, Y. *Langmuir* **2010**, *26*, 10778–10783.

(47) Levin, Y.; dos Santos, A. P. *J Phys: Cond Matt* **2014**, *26*, 203101.

(48) Kathmann, S. M.; Kuo, I.-F. W.; Mundy, C. J.; Schenter, G. K. *J Phys Chem B* **2011**, *115*, 4369–4377.

(49) Gopalakrishnan, S.; Liu, D.; Allen, H. C.; Kuo, M.; Shultz, M. J. *Chem Rev* **2006**, *106*, 1155–1175.

(50) Tong, Y.; Wirth, J.; Kirsch, H.; Wolf, M.; Saalfrank, P.; Campen, R. K. *J Chem Phys* **2015**, *142*, 054704.

(51) Tong, Y.; Vila Verde, A.; Campen, R. K. *J Phys Chem B* **2013**, *117*, 11753–11764.

(52) Bain, C. D.; Davies, P. B.; Ong, T. H.; Ward, R. N.; Brown, M. A. *Langmuir* **1991**, *7*, 1563–1566.

(53) Zhuang, X.; Miranda, P. B.; Kim, D.; Shen, Y. R. *Phys Rev B* **1999**, *59*, 12632–12640.

Electronic Supplementary Information for Experimentally Quantifying Anion Polarizability at the Air/Water Interface

VSF Spectra of 0.6 M Perchlorate Salt Solutions

I_{sf} is plotted as a function of incident infrared frequency for an 0.6 M solution of $NaClO_4$ in Figure S1. Clearly this solution also has a distinct ν_1 mode. Comparison with the spectra plotted in Figure 1 in the manuscript suggests that the break in symmetry that makes ν_1 IR active near the interface is not the result of an interfacial change in pKa.

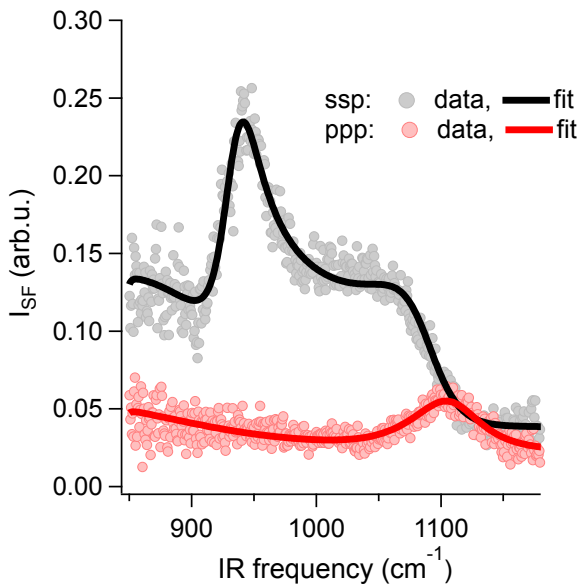

Figure S1: I_{sf} spectrum of an 0.6 M $NaClO_4$ solution plotted as a function of IR frequency. Clearly the spectrum, and the intensity of the ν_1 mode, is quantitatively similar to that for an $HClO_4$ solution (shown in the manuscript).

Line Shape Analysis Details & Full Results

We do a line shape analysis of our experimental data by performing a global fit of spectra – using the Levenberg-Marquardt algorithm as implemented in the commercial graphing and

analysis program Igor Pro (Wavemetrics) – collected under the *ssp* and *ppp* polarization conditions for all bulk $HClO_4$ concentrations using the line shape expression described in the text. To quantitatively account for the effect of the, finite, visible pulse spectral width we additional convolve this response with a gaussian of width $\Delta\nu_{800}$. The spectrum of the visible pulse is independently measured before each VSF measurement. To do the fit we assume a libration (of interfacial water) whose center frequency and line width we have determined in our previous study[1] and further assume, for concentrations lower than 1 M $HClO_4$, that the center frequencies and damping constants of the ν_1 and ν_3 modes; the libration amplitude; and the nonresonant amplitude and phase are all independent of concentration. Uncertainties reported with each fit parameter are calculated from a linearization of the model, with respect to its parameters, near the best fit. All results are shown in Tables S1 and S2.

Table S1: Results of fits to data collected employing the *ssp* polarization condition. The parameters shown in this and Table S2 are the result of a global fit to *ppp* and *ssp* spectra at all concentrations of $HClO_4$. Note that the spectral width of the 800 nm pulse was independently measured before each VSF measurement and the libration center frequency and line width were extracted from our previous work.[1]

$[HClO_4]$	(mol/L)	0	0.1	0.2	0.3	0.4	0.5	0.6	0.8
χ_{nr}						0.34 ± 0.07			
ϵ	(rad)					4.55 ± 0.13			
$\Delta\nu_{800}$	(cm^{-1})					12.2			
χ_{ν_1}		0	1.32 ± 0.1	2.03 ± 0.1	2.41 ± 0.2	2.69 ± 0.1	2.73 ± 0.1	2.91 ± 0.3	3.23 ± 0.2
$\tilde{\nu}_{\nu_1}$	(cm^{-1})					935 ± 1.0			
Γ_{ν_1}	(cm^{-1})					12.1 ± 0.7			
χ_{ν_3}		0	-2.44 ± 1.6	-5.71 ± 0.4	-6.28 ± 1.0	-6.56 ± 0.9	-7.98 ± 0.37	-8.03 ± 1.1	-8.14 ± 1.4
$\tilde{\nu}_{\nu_3}$	(cm^{-1})					1110 ± 1.4			
Γ_{ν_3}	(cm^{-1})					35.7 ± 1.2			
χ_{lib}						17.83 ± 4.2			
$\tilde{\nu}_{lib}$	(cm^{-1})					832			
$\Gamma_{lib\nu_3}$	(cm^{-1})					135			

The *ppp* spectra corresponding to the *ssp* spectra shown in Figure 2 in the manuscript are shown in Figure S2. Clearly this signal is weak. However, we are interested in extracting the amplitude of the ν_1 mode subject to the constraints described above. Given these boundary conditions we find, as is hopefully clear from inspection of the data, that a nonzero *ppp* amplitude exists at all $HClO_4$ concentrations 0.2 M and above. While we globally fit all data

Table S2: Results of fits to data collected employing the *ppp* polarization condition. The parameters shown in this and Table S1 are the results of a global fit to *ppp* and *ssp* spectra at all concentrations of $HClO_4$. Note that the spectral width of the 800 nm pulse was independently measured before each VSF measurement and the libration center frequency and line width were extracted from our previous work.[1]

$[HClO_4]$	(mol/L)	0	0.1	0.2	0.3	0.4	0.5	0.6	0.8
χ_{nr}						0.34 ± 0.05			
ϵ	(rad)					4.55 ± 0.15			
$\Delta\nu_{800}$	(cm^{-1})					12.2			
χ_{ν_1}		0	0.04 ± 0.1	0.25 ± 0.1	0.26 ± 0.1	0.27 ± 0.1	0.25 ± 0.1	0.24 ± 0.1	0.26 ± 0.1
$\tilde{\nu}_{\nu_1}$	(cm^{-1})					935 ± 2.3			
Γ_{ν_1}	(cm^{-1})					12.1 ± 0.6			
χ_{ν_3}		0	-2.80 ± 1.6	-2.37 ± 0.4	-5.52 ± 1.0	-6.49 ± 0.9	-6.98 ± 0.37	-7.21 ± 1.1	-7.14 ± 1.4
$\tilde{\nu}_{\nu_3}$	(cm^{-1})					1110 ± 0.7			
Γ_{ν_3}	(cm^{-1})					35.7 ± 0.9			
χ_{lib}						17.83 ± 0.7			
$\tilde{\nu}_{\mathrm{lib}}$	(cm^{-1})					832			
$\Gamma_{\mathrm{lib}\nu_3}$	(cm^{-1})					135			

sets to extract the center frequencies of ν_1 and ν_3 the relatively weak ν_1 amplitude, differing noise at the low frequency side of the measurement, and the coherent nature of the VSF response (leading to interference with the ν_3), leads to small frequency shifts in the apparent peak in the signal even as the data is well described by a constant resonance frequency.

The Raman Depolarization Ratio in Bulk and at the Interface

In the following section we develop the full description of the connection between the Raman depolarization ratio and measured VSF intensities as described in the literature by Long and Hirose et al[2,3] and recently reviewed by Wang et al.[4] Given a ClO_4^- ion has $C_{3\nu}$ symmetry, assuming off diagonal terms in the polarizability tensor are small and the c-axis is taken along the rotational symmetry axis of the ion, there are three nonzero and two independent terms in the polarizability tensor: $\alpha_{aa} = \alpha_{bb}$, α_{cc}. For this molecule the Raman depolarization ratio is defined (where $R = {}^{\alpha_{aa}}/_{\alpha_{cc}}$):

$$\rho = \frac{I_\perp}{I_\parallel} = \frac{3(\alpha_a)^2}{45(\alpha_i)^2 + 4(\alpha_a)^2} = \frac{3}{4 + 5\left[(1+2R)/(R-1)\right]^2} \tag{S1}$$

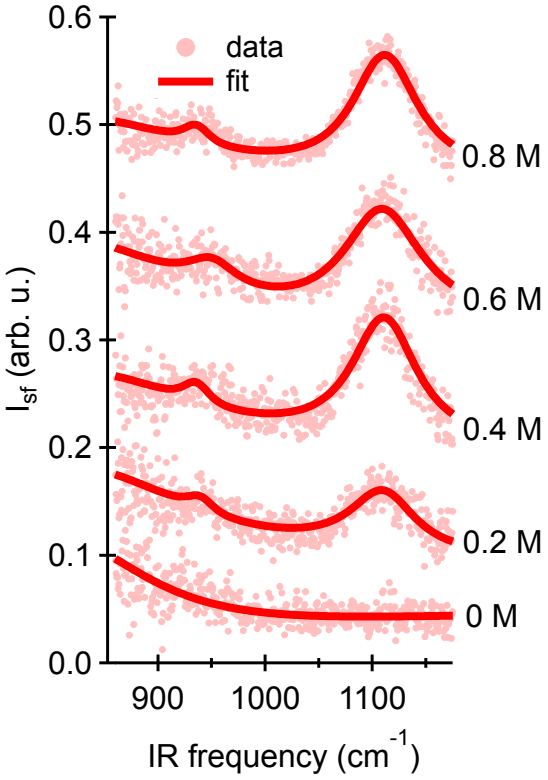

Figure S2: VSF spectra plotted as a function of bulk concentration of $HClO_4$ collected under the *ppp* polarization condition. Lines shown on the data are the results of global fits including the *ssp* data shown in Figure 2 in the manuscript.

α_i is defined,

$$\alpha_i = {}^1\!/_3\,(\alpha_{aa} + \alpha_{bb} + \alpha_{cc}) \tag{S2}$$

and α_a is defined,

$$(\alpha_a)^2 = {}^1\!/_2\left[(\alpha_{aa} - \alpha_{bb})^2 + (\alpha_{bb} - \alpha_{cc})^2 + (\alpha_{cc} - \alpha_{aa})^2 + 6(\alpha_{ab}^2 + \alpha_{bc}^2 + \alpha_{ca}^2)\right] \tag{S3}$$

Clearly, then, if we could extract R with interfacial specificity we could define an *interfacial* Raman depolarization ratio.

As has been described extensively in the literature[5] the measured VSF intensity, *i.e.* $\mathrm{I_{sf}}$, collected in reflection at the air/water interface can be written:

$$\mathrm{I_{sf}} = \frac{8\pi^3\omega_{\mathrm{sf}}^2 \sec^2\gamma_{\mathrm{sf}}}{c^3}\left|\chi_{\mathrm{eff}}^{(2)}\right|^2 \mathrm{I_{vis}I_{ir}} \tag{S4}$$

in which γ_i is the angle of beam i with respect to the surface normal, ω_i is the frequency of field i, c is the speed of light, I_i is the intensity of field i and $\chi_{\mathrm{eff}}^{(2)}$ is the effective, macroscopic, nonlinear susceptibility of the air/water interface. $\chi_{\mathrm{eff}}^{(2)}$ is a function of the nonlinear Fresnel factors (L_{ij}) and the polarizations of the incident and outgoing fields. These relationships can be written (assuming z is along the surface normal and x, y the plane of the surface),

$$\chi_{\mathrm{eff},ssp}^{(2)} = L_{yy}(\omega_{\mathrm{sf}})L_{yy}(\omega_{\mathrm{vis}})L_{zz}(\omega_{\mathrm{ir}})\sin\gamma_{\mathrm{ir}}\chi_{yyz}^{(2)} \tag{S5}$$

$$\begin{aligned}\chi_{\mathrm{eff},ppp}^{(2)} = {} & -L_{xx}(\omega_{\mathrm{sf}})L_{xx}(\omega_{\mathrm{vis}})L_{zz}(\omega_{\mathrm{ir}})\cos\gamma_{\mathrm{sf}}\cos\gamma_{\mathrm{vis}}\sin\gamma_{\mathrm{ir}}\chi_{xxz}^{(2)} \\ & -L_{xx}(\omega_{\mathrm{sf}})L_{zz}(\omega_{\mathrm{vis}})L_{xx}(\omega_{\mathrm{ir}})\cos\gamma_{\mathrm{sf}}\sin\gamma_{\mathrm{vis}}\cos\gamma_{\mathrm{ir}}\chi_{xzx}^{(2)} \\ & +L_{zz}(\omega_{\mathrm{sf}})L_{xx}(\omega_{\mathrm{vis}})L_{xx}(\omega_{\mathrm{ir}})\sin\gamma_{\mathrm{sf}}\cos\gamma_{\mathrm{vis}}\cos\gamma_{\mathrm{ir}}\chi_{zxx}^{(2)} \\ & +L_{zz}(\omega_{\mathrm{sf}})L_{zz}(\omega_{\mathrm{vis}})L_{zz}(\omega_{\mathrm{ir}})\sin\gamma_{\mathrm{sf}}\sin\gamma_{\mathrm{vis}}\sin\gamma_{\mathrm{ir}}\chi_{zzz}^{(2)}\end{aligned} \tag{S6}$$

The nonlinear Fresnel factors are a function of the bulk and interfacial refractive indices and

beam angles,

$$L_{xx}(\omega_i) = \frac{2n_{\text{air}}(\omega_i)\cos\zeta_i}{n_{\text{air}}(\omega_i)\cos\zeta_i + n_{\text{water}}(\omega_i)\cos\gamma_i} \tag{S7}$$

$$L_{yy}(\omega_i) = \frac{2n_{\text{air}}(\omega_i)\cos\gamma_i}{n_{\text{air}}(\omega_i)\cos\gamma_i + n_{\text{water}}(\omega_i)\cos\zeta_i} \tag{S8}$$

$$L_{zz}(\omega_i) = \frac{2n_{\text{water}}(\omega_i)\cos\gamma_i}{n_{\text{air}}(\omega_i)\cos\beta_i + n_{\text{water}}(\omega_i)\cos\gamma_i}\left(\frac{n_{\text{air}}(\omega_i)}{n'(\omega_i)}\right)^2 \tag{S9}$$

in which ζ_i is the refracted angle of beam i (*i.e.* $n_{\text{air}}(\omega_i)\sin\gamma_i = n_{\text{water}}(\omega_i)\sin\zeta_i$), n_i is the, frequency dependent, refractive index of bulk phase i, and n' is the, also frequency dependent, refractive index of the interface. The material nonlinear susceptibility in the lab frame, *i.e.* $\chi^{(2)}_{ijk}$, can be expressed in terms of the nonlinear molecular response, and the ensemble averaged orientation of ions with a $C_{3\nu}$ symmetry symmetric stretch as:

$$\chi^{(2)}_{zzz} = N_s\beta^{(2)}_{ccc}\left[R\langle\cos\theta\rangle + \langle\cos^3\theta\rangle(1-R)\right] \tag{S10}$$

$$\chi^{(2)}_{xxz} = \chi^{(2)}_{yyz} = {}^1\!/\!_2 N_s\beta^{(2)}_{ccc}\left[\langle\cos\theta\rangle(1+R) - \langle\cos^3\theta\rangle(1-R)\right] \tag{S11}$$

$$\begin{aligned}\chi^{(2)}_{xzx} &= \chi^{(2)}_{yzy} = \chi^{(2)}_{zxx} = \chi^{(2)}_{zyy} \\ &= {}^1\!/\!_2 N_s\beta^{(2)}_{ccc}(1-R)\left[\langle\cos\theta\rangle - \langle\cos^3\theta\rangle\right]\end{aligned} \tag{S12}$$

in which $\beta^{(2)}_{abc}$ is the hyperpolarizability (*i.e.* the molecular nonlinear response), the c-axis is the rotational symmetry of the $C_{3\nu}$ molecule, θ is the orientation of the ClO_4^- with respect to the surface normal (the z-axis) and $R = {}^{\beta^{(2)}_{aac}}\!/\!_{\beta^{(2)}_{ccc}}$.

In this study we employed incident beams in the visible and infrared. These frequencies were chosen such that the infrared is resonant with Cl-O vibrations and the visible is nonresonant. Under such conditions $\beta^{(2)}$ is an anti-stokes scattering from an IR induced polarization:

$$\beta^{(2)}_{ijk} = \frac{1}{2\hbar}\frac{\alpha_{ij}\mu_k}{(\omega_n - \omega_{\text{ir}} - i\Gamma_n)} \tag{S13}$$

in which $\hbar$ is the reduced Planck's constant, ω_n is the center frequency of the nth vibration,

ω_{ir} is the frequency of the incident ir, Γ_n is the damping constant of the nth mode, α_{ij} is the polarizability tensor (as described in equations S2-S3) and μ_k is the transition dipole. Given equation S13, substituting equations S10, S11 and S12 and equations S7, S8 and S9 into equations S5 and S6 suggests that, if we know the orientation of the ClO_4^- and measure I_{sf} under the *ppp* and *ssp* polarization conditions, the $^{ppp}/_{ssp}$ ratio depends only on R. Because $\beta^{(2)}$ is a product of the polarizability and transition dipole:

$$R = \frac{\beta^{(2)}_{aac}}{\beta^{(2)}_{ccc}} = \frac{\alpha_{aa} \times \mu_c}{\alpha_{cc} \times \mu_c} = \frac{\alpha_{aa}}{\alpha_{cc}} \tag{S14}$$

Equation S14 thus implies that by taking the ratio of I_{sf} measured under the *ppp* and *ssp* polarization conditions we can extract an R for interfacial ClO_4^- and calculate an interfacial Raman depolarization ratio.

Evaluating Assumptions in the Calculation of Interfacial ρ

What is the dependence of calculated ρ on ClO_4^- orientation?

Given the set of equations shown, an experimentally measured $\chi_r^{ssp}/\chi_r^{ppp}$ ratio, and assuming a ClO_4^- orientation one can extract a value of R. The resulting solution is plotted in Figure S3. Calculated interfacial values of ρ shown in the manuscript assume the ClO_4^- anion is oriented between 0 and 45° and R values range between 0 and 1. Orientations between 45 and 90 degrees would imply ion pairing and (further) reduced ClO_4^- symmetry for which we see no spectral evidence. R values above 2 imply that the ν_1 polarizability is larger perpendicular to the Cl-O bond than parallel. Prior experiment and theory has shown that this is not the case in bulk.[6] Our electronic structure calculations suggests that this is not the case for ClO_4^- in an applied field similar in amplitude to what we would expect in the local interfacial environment.

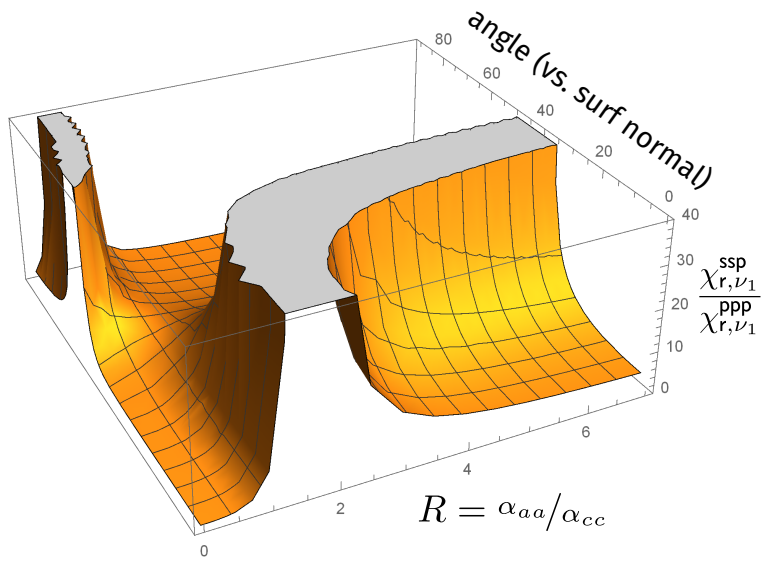

Figure S3: Calculated relationship of the R at the IR frequencies of the ν_1 mode, measured $\chi^{ssp}_{r,\nu_1}/\chi^{ppp}_{r,\nu_1}$ and ClO_4^- orientation. The physically relevant solution to this set of equations is that with an R value between 0 and 1.

Is ClO_4^- orientation concentration dependent?

The transition dipole of the ν_1 and ν_3 modes of the ClO_4^- anion are orthogonal. One consequence of this property is that changes in interfacial orientation of the ClO_4^- anion will result in changes in relative intensities of the ν_1 and ν_3 modes as a function of bulk $HClO_4$ orientation (for resonances appearing in spectra collected under a single polarization condition). The calculated dependence of the $\chi^{ssp}_{r,\nu_3}/\chi^{ssp}_{r,\nu_1}$ are shown in Figure S4 and the experimentally measured values, repeated from Figure 2 in the manuscript for ease of comparison, in Figure S5. Comparison of the two figures makes clear that, if ClO_4^- orientation changes as a function of bulk concentration of $HClO_4$ (and thus presumably with increasing *interfacial* ClO_4^- concentration), this orientation change must be small.

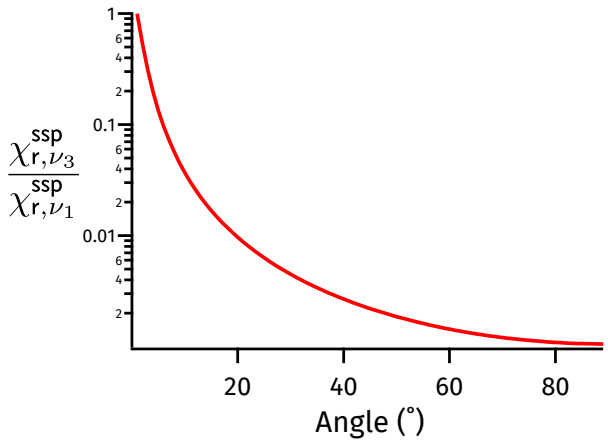

Figure S4: Calculated $\chi^{ssp}_{r,\nu_3}/\chi^{ssp}_{r,\nu_1}$ ratio as a function of ClO_4^- orientation. Clearly even few degree changes in orientation should lead to large changes in ratio.

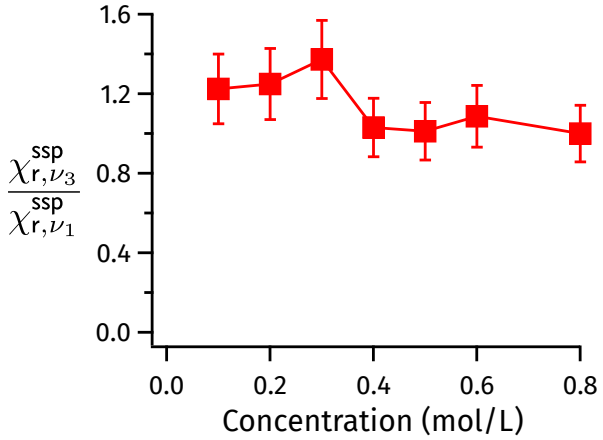

Figure S5: Ratios of $\chi^{ssp}_{r,\nu_3}/\chi^{ssp}_{r,\nu_1}$ extracted from experiment for spectra collected under the *ssp* polarization condition. Clearly comparison of experiment with the calculated result shown in Figure S4 suggest that ClO_4^- orientation is relatively insensitive to bulk $HClO_4$ orientation.

Computational Details

Methods

We simulated the deformation of an isolated ClO_4^- anion exposed to external electric dipole fields along the z-axis and studied the resulting changes of the dipole moment and the related Raman depolarization ratio. Three popular density functional approximations, *i.e.* PBEPBE,[7] PBE0[8] and B3LYP,[9] were employed together with a series of Gaussian-type basis sets, (aug-)cc-pVnZ with n=T, Q, 5. The calculations were performed using the GAMESS package.[10] As shown in Tables S3-S10, the three methods predict a very similar influence of the external electric dipole fields on the ClO_4^- anion, with a slight method-dependent discrepancy in the calculated Cl-O bond length.

Results

Table S3: Results employing the approach described above using the PBEPBE/cc-pVTZ model chemistry.

E_z (Debye)	ϕ_z (meV)	Dipole	ρ	Cl-O_z (Å)	Cl-O_{other} (Å)	Angle	Cl-O_z/Cl-O_{other}	IR intens
0	0	0.0001	0.0000	1.4916	1.4916	109.47	1.00	0.0001
0.0127	136.06	-0.2316	0.0003	1.5021	1.4884	108.96	1.01	3.403
0.0254	272.11	-0.4672	0.0018	1.5138	1.4852	108.46	1.02	17.68
0.0381	408.17	-0.7089	0.0056	1.5275	1.4820	107.94	1.03	50.59
0.0508	544.23	-0.9575	0.0124	1.5434	1.4788	107.44	1.04	103.1

Table S4: Results employing the approach described above using the PBEPBE/aug-cc-pVTZ model chemistry.

E_z (Debye)	ϕ_z (meV)	Dipole	ρ	Cl-O_z (Å)	Cl-O_{other} (Å)	Angle	Cl-O_z/Cl-O_{other}	IR intens
0	0	0.0001	0.0000	1.4954	1.4954	109.47	1.00	0.0002
0.0127	136.06	-0.3041	0.0013	1.5074	1.4919	108.96	1.01	7.004
0.0254	272.11	-0.6242	0.0082	1.5222	1.4882	108.40	1.02	43.15
0.0381	408.17	-0.9588	0.0251	1.5397	1.4844	107.88	1.04	125.6
0.0508	544.23	-1.302	0.0450	1.5603	1.4807	107.31	1.04	229.2

Table S5: Results employing the approach described above using the PBEPBE/aug-cc-pVQZ model chemistry.

E_z (Debye)	ϕ_z (meV)	Dipole	ρ	Cl-O_z (Å)	Cl-O_{other} (Å)	Angle	Cl-O_z/Cl-O_{other}	IR intens
0	0	0.0001	0.0000	1.4831	1.4831	109.47	1.00	0.0002
0.0127	136.06	-0.3015	0.0011	1.4946	1.4797	108.96	1.01	6.572
0.0254	272.11	-0.6160	0.0077	1.5086	1.4758	108.46	1.02	42.05
0.0381	408.17	-0.9482	0.0238	1.5248	1.4722	107.93	1.04	124.4
0.0508	544.23	-1.312	0.0417	1.5452	1.4687	107.37	1.05	238.3

Table S6: Results employing the approach described above using the PBEPBE/aug-cc-pV5Z model chemistry.

E_z (Debye)	ϕ_z (meV)	Dipole	ρ	Cl-O_z (Å)	Cl-O_{other} (Å)	Angle	Cl-O_z/Cl-O_{other}	IR intens
0	0	0.0001	0.0000	1.4731	1.4731	109.47	1.00	0.0002
0.0127	136.06	-0.2982	0.0011	1.4845	1.4694	108.98	1.01	7.050
0.0254	272.11	-0.6076	0.0074	1.4978	1.4660	108.48	1.02	41.95
0.0381	408.17	-0.9369	0.0237	1.5137	1.4625	107.96	1.04	128.3
0.0508	544.23	-1.298	0.0392	1.5328	1.4590	107.41	1.05	249.7

Table S7: Results employing the approach described above using the B3LYP/aug-cc-pVTZ model chemistry.

E_z (Debye)	ϕ_z (meV)	Dipole	ρ	Cl-O_z (Å)	Cl-O_{other} (Å)	Angle	Cl-O_z/Cl-O_{other}	IR intens
0	0	0.0001	0.0000	1.4789	1.4789	109.47	1.00	0.0001
0.0127	136.06	-0.2878	0.0011	1.4909	1.4755	108.96	1.01	6.768
0.0254	272.11	-0.5818	0.0066	1.5037	1.4720	108.45	1.02	37.19
0.0381	408.17	-0.8911	0.0215	1.5195	1.4686	107.91	1.03	109.1
0.0508	544.23	-1.219	0.0437	1.5378	1.4651	107.36	1.05	204.6

Table S8: Results employing the approach described above using the B3LYP/aug-cc-pV5Z model chemistry.

E_z (Debye)	ϕ_z (meV)	Dipole	ρ	Cl-O_z (Å)	Cl-O_{other} (Å)	Angle	Cl-O_z/Cl-O_{other}	IR intens
0	0	-0.0001	0.0000	1.4572	1.4572	109.47	1.00	0.0001
0.0127	136.06	-0.2651	0.0009	1.4680	1.4538	108.99	1.01	6.892
0.0254	272.11	-0.5390	0.0063	1.4807	1.4506	108.49	1.02	41.12
0.0381	408.17	-0.8244	0.0205	1.4951	1.4473	107.99	1.03	119.6
0.0508	544.23	-1.132	0.0415	1.5127	1.4437	107.46	1.05	230.6

Table S9: Results employing the approach described above using the PBE0/aug-cc-pVTZ model chemistry.

E_z (Debye)	ϕ_z (meV)	Dipole	ρ	Cl-O_z (Å)	Cl-O_{other} (Å)	Angle	Cl-O_z/Cl-O_{other}	IR intens
0	0	0.0001	0.0000	1.4620	1.4620	109.47	1.00	0.0141
0.0127	136.06	-0.2737	0.0008	1.4722	1.4589	108.98	1.01	6.315
0.0254	272.11	-0.5552	0.0054	1.4840	1.4558	108.49	1.02	36.47
0.0381	408.17	-0.8460	0.0176	1.4973	1.4528	107.99	1.03	103.4
0.0508	544.23	-1.150	0.0377	1.5124	1.4496	107.47	1.04	197.6

Table S10: Results employing the approach described above using the PBE0/aug-cc-pV5Z model chemistry.

E_z (Debye)	ϕ_z (meV)	Dipole	ρ	Cl-O_z (Å)	Cl-O_{other} (Å)	Angle	Cl-O_z/Cl-O_{other}	IR intens
0	0	-0.0001	0.0000	1.4437	1.4437	109.47	1.00	0.0003
0.0127	136.06	-0.2538	0.0007	1.4537	1.4408	109.01	1.01	5.870
0.0254	272.11	-0.5151	0.0048	1.4651	1.4379	108.53	1.02	34.85
0.0381	408.17	-0.7857	0.0166	1.4779	1.4349	108.05	1.03	104.6
0.0508	544.23	-1.070	0.0359	1.4921	1.4316	107.56	1.04	207.6

Solutions with Concentrations > 1 M $HClO_4$

I_{sf} spectra of 2, 5 and 11.6 M solutions of $HClO_4$ are shown in Figure S6. These higher concentration spectra show a clear shift in the maximum of the spectral response associated with the ν_3 mode and a gain in intensity between the ν_1 and ν_3. These trends are consistent with the splitting of ν_3 expected under conditions in which T_d symmetry is lifted. A similar gain in intensity at frequencies between the ν_1 and ν_3 modes has been previously observed in Raman spectra of aqueous $HClO_4$ solutions above 16 M and assigned to ion pairing or the appearance of molecular acid. Quantitative analysis suggests that these phenomena occur in *interfacial* ClO_4^- at concentrations more than 10× lower that in bulk.

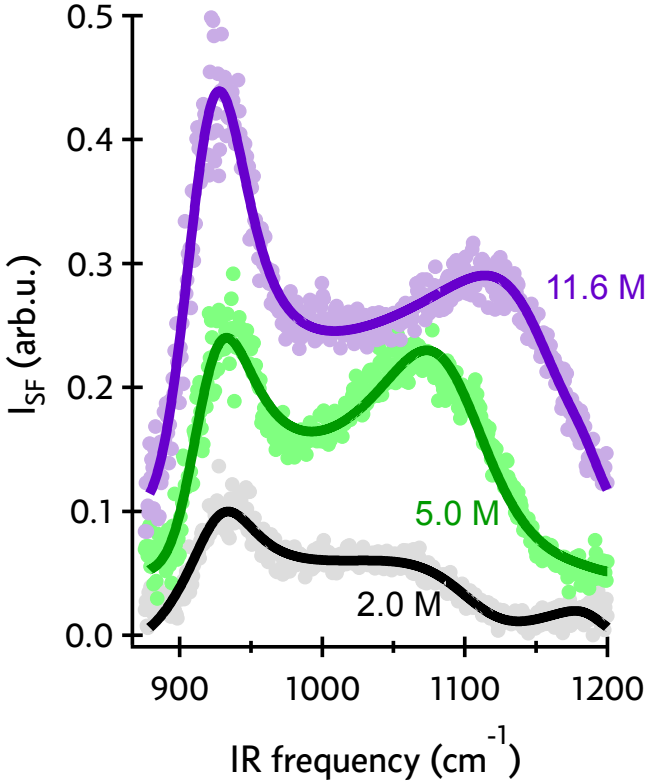

Figure S6: VSF spectra of bulk $HClO_4$ solutions of 2, 5 and 11.6 M collected under the *ssp* polarization condition. Dot are data, the solid lines are fits. In order to describe the data using the line shape model described above we found it necessary to introduce an additional resonance. Clearly, when comparing these data to those shown in Figure 1 in the manuscript, with increasing concentration the ν_3 mode appears to split at sufficiently high concentration. Spectra are offset for clarity.

References

(1) Tong, Y.; Kampfrath, T.; Campen, R. K. *Phys Chem Chem Phys* **2016**, *18*, 18424–18430.

(2) Long, D. A. *The Raman Effect: A Unified Treatment of the Theory of Raman Scattering by Molecules*; Wiley, 2001.

(3) Hirose, C.; Akamatsu, N.; Domen, K. *J Chem Phys* **1992**, *95*, 997–1004.

(4) Wang, H.; Gan, W.; Lu, R.; Rao, Y.; Wu, B.-H. *Int Rev Phys Chem* **2005**, *24*, 191–256.

(5) Lambert, A. G.; Davies, P. B.; Neivandt, D. J. *Appl Spect Rev* **2005**, *40*, 103–145.

(6) Hyodo, S.-a. *Chem Phys Lett* **1989**, *161*, 245–248.

(7) Perdew, J.; Burke, K.; Ernzerhof, M. *Phys Rev Lett* **1996**,

(8) Perdew, J. P.; Ernzerhof, M.; Burke, K. *J Chem Phys* **1996**, *105*, 9982–9985.

(9) Becke, A. D. *J Chem Phys* **1993**, *98*, 5648–5652.

(10) Schmidt, M. W.; Baldridge, K. K.; Boatz, J. A.; Elbert, S. T.; Gordon, M. S.; Jensen, J. H.; Koseki, S.; Matsunaga, N.; Nguyen, K. A.; Su, S.; Windus, T. L.; Dupuis, M.; Montgomery Jr, J. A. *J Comput Chem* **1993**, *14*, 1347–1363.